Constrained Systems: Caught between Dimensions

René M. Overney and Scott E. Sills

Department of Chemical Engineering, University of Washington, Box 351750, Seattle, WA 98195

This chapter discusses the problematic nature of interfacial sciences when constrained to the mesoscale. Interfacial sciences are trapped between the atomistic and the three-dimensional bulk regimes – the mesoscale. We experience a breakdown of phenomenological descriptions used to characterize macrosystems. Furthermore, submicrometer systems with their fractal-like dimension cannot be adequately described with quantum or molecular interaction theories. The challenge of describing the mesoscale for the various scientific fields is to find a common denominator. By suggesting a possible classification of the field and by discussing examples in each category, this chapter attempts to illuminate the similarities of mesoscale properties obtained in different research and engineering disciplines.

Since mathematicians have introduced us to many dimensions, it has been our desire to strive for more degrees of freedom while seemingly unsatisfied with the three dimensions we live in. Our pursuit of entertaining ourselves with fictions that escape our common senses is documented as early as 1884 in the satire "Flatland - A Romance of Many Dimensions" by Edwin A. Abbott.[1] While Abbott's work tries to introduce the reader to the concept of the multi-dimensional space, it chooses fewer dimensions than three as starting point. By doing so, Abbott came up with imaginary laws of nature that apply in one and two dimensions. Although these laws, which for instance explain how rain is experienced in two dimensions, are unrealistic, they impressively illustrate the mystery of lower dimensionalities.

Indeed, the laws of nature, or more appropriately, the perception of them in the form of material and transport properties, are challenged if a three dimensional bulk material is reduced to a two dimensional plane. This becomes apparent in many interfacial applications, such as thin film technologies. Structural, material, and transport properties are increasingly dominated by interfacial, interactive, and dimensional constraints. Statistical properties are altered in small ensemble systems, and interfacial properties become dominant on the so-called *mesoscale*.

This introductory chapter is intended to provide an overview of the field, and Table 1 will be utilized as a guide to classify the various aspects of interfacial sub-microscale properties. An alternate system classification would have been in terms of steady-state and transient thermodynamics. Unfortunately, many available interpretations of experimental data obtained on the mesoscale are disputable regarding their distinction between equilibrated properties and apparent transient properties.

Table 1: Classification of Various Aspects of Interfacial Sub-microscale Properties.

Structural, Material, and Transport Properties			
Dimensional Effects on Properties	**Small Ensemble Systems**	**Constrained Systems**	**Critical Length Scales, Kinematics, & Dissipation**
Property equations solved in 1D, 2D or 3D lead to different solutions.	Statistical mechanics fails to predict exotic properties.	Properties are affected by internal or interfacial constraints.	Processes are affected by dimensional limitations.
e.g., Rayleigh surface waves vs. Huygen's body wave	e.g., exciton annihilation in ultrathin films	e.g., interfacial constraints in ultrathin films	e.g., friction as an interfacial process

The Reader will find each category of Table 1 discussed in the following sections of this chapter. The first section provides some brief general remarks about properties supported by an illustrative example that would have fit well into Abbott's satirical novel on how the perception of properties are characterized by the dimensionality of the governing equation. Small ensembles and size effects are discussed in the succeeding section. Particularly emphasized in the second section are optoelectronic properties and quantum confinement. The third section deals with interfacially constrained systems and discusses structural changes at interfaces and their effect on viscoelastic and thermal material properties. Specific emphasis is placed on thin polymeric and interfacially trapped fluidic systems. Finally, the fourth section introduces the terminology of critical time and length scales, and discusses the effect of dimensional limitations on processes such as friction.

Remarks about Material and Transport Properties

Material properties, either physical or chemical in nature, are distinctive attributes of a steady-state condensed system. It is imposed that such *intrinsic* properties are time independent, i.e., they describe thermodynamically equilibrated material characteristics.

An experimentally determined value is referred to as an *apparent property value* if it depends on system parameters, for instance, the rate at which the experiment is performed. An example of a rate dependent property is viscosity. By

definition, the intrinsic value of a rate dependent property is the extrapolated value in regards of an infinite time period over which the property is obtained. There are properties that are combinations of truly independent properties, e.g., the material density as the mass per unit volume. The properties of foremost interest are *intensive* properties, i.e., properties that are independent of the size of a system.

Transport properties such as wave propagation, diffusion, and conduction are known to depend strongly on material properties, but also on geometrical constraints and dimensional confinement. It is very challenging, especially in mesoscopic systems like ultrathin films, to determine the origin for exotic, not bulk-like, transport properties.

Let us consider a well-known example where transport properties are significantly dissimilar for different dimensionalities; that is the energy transport described by the wave equation, i.e.:

$$\Delta_N u = c^2 \frac{\partial^2 u}{\partial t^2}; \quad u = u(\vec{x}, t); \quad \vec{x} = (x_1, x\ ..., x_N). \quad (1)$$

It is well known that the qualitative time behavior of the solution, *u*, of the wave equation is significantly different for a three dimensional wave propagation, N=3, compared to a one or two dimensional system, N = 1 or 2. For N=3, a spatially localized initial disturbance gives rise to a time limited disturbance only, at any accessible location away from the source of the disturbance. This is different for N=1 or 2, where the disturbance is for all times noticeable at any accessible location if there are no dissipative effects.

The moving wave propagations in three dimensions have well defined tailing and front border wave fronts that we experience daily by speaking with each other or by listening to radio transmissions. We would not be able to communicate in the same manner in a two dimensional world with surface waves. Lord Rayleigh discovered that waves propagating over the surface of a body with a small penetration distance into the interior of the body, travel with a velocity independent of the wave-length and slightly smaller than the velocity of equivoluminal waves propagating through the body.[2] It has been found that the so-called Rayleigh waves, which diverge in two-dimensions only, acquire a continually increasing preponderance at great distances from the source. This two dimensional effect of wave propagation has been found to be very important in the study of seismic phenomena.[3]

Small Ensembles and Size Effects

Quantum Confinement

Phenomenological theories fail to describe transport and material properties of small ensemble systems, i.e., systems in which the number of molecules is smaller than Avogadro's number. Within the last century, it has been theoretically predicted and experimentally confirmed that small ensemble systems generate some sort of quantum confinement, in which optoelectronic, electronic, and magnetic wave propagation experience quantized nanoscale size effects.

It has been found that size limited materials such as particles, films, and composites, synthesized with nanometer dimensions can exhibit exotic quantized properties. For instance, altered phenomena in emission lifetime, luminescence quantum efficiency, and concentration quenching have been reported with nanoparticle-doped systems.[4-9] In various doped nanocrystalline (DNC) phosphors, ZnS:Mn and ZnS:Tb, quantum confinement effects were found for doping particles with critical dimensions below 5 nm resulting in shortening of the luminescence lifetime by several orders of magnitude.[10] The origin of these quantum confinement effects is postulated to arise from mixing of s-p and d-f electrons from the host with the valence band of the activator leading to forbidden d-d and f-f transitions.[10] Theoretical predictions are still sparse due to the inadequate experimental database. One of the few theoretical predictions suggests that the electron-phonon interactions are modified on the nanometer scale.[11] This is supported by experiments in semiconducting nanoparticles which claim growth rates inversely proportional to the square of particle diameter ($\sim 1/d^2$).[12,13] With site-selective optical spectroscopy, where lanthanide emitters serve as sensitive probes of nanostructured materials, quantum confinement effects are utilized to determine material properties such as the degree of disorder or crystallinity, phase transformations and distributions, phonon spectra, and defect chemistry.[4,14,15].

Interfacially induced Pseudo-Quantum Confinement in Optoelectronic Devices

Outside the quantum-well distance of about 10 nm or even less, it is expected that the materials exhibit bulk-like properties. However, in a recent study by Jenekhe and coworkers, it has been shown that the electroluminescence (EL) wave length of a binary ultrathin polymer film exhibits very unique properties that could be attributed to an unexpected quantum effect.[9]

The origin of the EL emission is provided by the formation of excitons, or electron-hole pairs, which are formed at defect sites, i.e. donor/acceptor sites, in the material and at the interface of a heterojunction of two semiconducting polymer layers. Little is known at this time about the mobility of the electrons, holes, and excitons at the interface of heterojunctions. Limited exciton diffusion lengths in the materials and the interfacial nature of the photogeneration process could explain these exotic transport properties in terms of topological constraints.

The experiment by Jenekhe and coworkers demonstrated that below a critical thickness of the semiconducting polymer structure, the optoelectronic device exhibits a three-fold

enhancement in the photoconductivity and allows for voltage-tunable reversible color changes, Figure 1.[9] These interfacially induced pseudo-quantum confinement effects have been observed for critical sizes (i.e., film thicknesses) up to at least 40 nm.

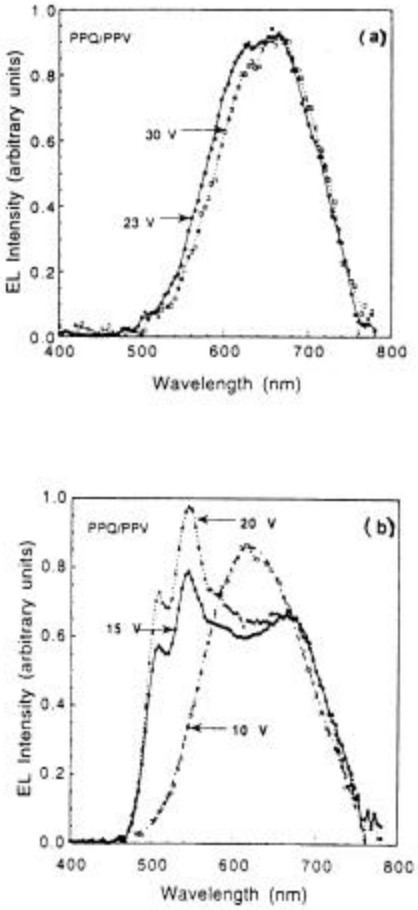

Figure 1. EL spectra of PPQ/PPV heterojunction devices with constant PPV thickness of 25 nm. (a) Voltage independent spectra for a PPQ film thickness of 67 nm. (b) Voltage dependent spectra for a PPQ film thickness of 40 nm. Reproduced with permission from reference 7. American Chemical Society, 1997.

The optoelectronic experiment is briefly described as follows: Two semiconducting films, n-type and p-type, were sandwiched between aluminum and indium-tin oxide (ITO) electrodes as illustrated in Figure 2. The n-type, electron transporting polymer layer consisted of polyquinolines (PPQ), and the p-type, hole transporting polymer layer consisted of p-phenylenes (PPV). The luminescence was measured as function of the film thickness of the polymers, and the applied voltage, Figure 1. The electroluminscent (EL) spectra were found dependent on the thickness of the PPQ n-type polymer layer.

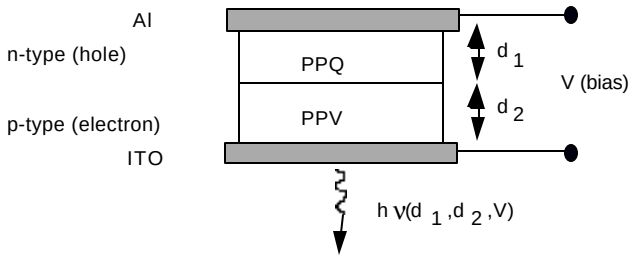

*Figure 2: EL junction of two semiconducting polymer films. The frequency, **n**, of the luminescence is found to be dependent on the bias voltage, V, for films with critical thickness d_1=40 nm and d_2=20 nm, respectively (see Figure 1). Note that the finite size distance is outside the expected quantum-well dimension (~10 nm) asking for mesoscale interpretations.*

For 67 nm thick PPQ films and 25 nm PPV p-type layer, the photoluminescence was found to be voltage independent over the range of 10-30 V and identical to a single-layer ITO-PPQ-AL device (orange/red), Figure 1(a). Significantly altered spectra were obtained for a reduced film thickness of PPQ from 67 nm to 40 nm, Figure 1(b). At low bias voltages ranging from 8-10 V, a unipolar hole transfer was observed leading to an orange emission that is characteristic of PPQ. At a higher voltage range of 13-20 V, a broadband spectra was obtained caused by a bipolar electron-hole transfer of both layers leading to a green color. The emission intensity could also be influenced for a PPQ film of constant thickness of 40 nm by varying the thickness of the p-type layer of PPV. In such a system, the intensity of the hole transport is controlled by the film thickness of PPV, and the electron transport is controlled with the voltage.[9]

Structurally Constrained Systems

Interfacially Confined Polymer Films

The "large" size effect that has been found in polymeric optoelectronic devices (see above) is not unique in polymer science. While materials such as ceramics, metals, oxides, exhibit size limitations only noticeable below 10 nm, quantum-well effects, it was found that in polymer systems, interfacial effects could be noticeable over distances of tens to hundreds of nanometers. Over the last few years, various groups reported bulk-deviating structural and dynamic properties for polymers at interfaces. [16-22] For instance, increased molecular mobility was observed at the free surface for thick films.[16] Reduced molecular mobility at the film surface of ultrathin films was reported based on forward recoil spectroscopy measurements.[17] In secondary ion mass spectrometry (SIMS) and scanning force microscopy (SFM) studies of graft-copolymers, it was found that the degree of molecular ordering significantly affects dynamic processes at

interfaces.[18] Self-organization of graft and block-copolymers at surfaces and interfaces were found with transmission electron microscopy(TEM) and neutron reflectivity(NR).[19-22]

Application of mean-field theories to interfacially constrained and size-limited polymer systems failed to describe the rather unexpected mesoscale behavior observed experimentally. The extension of the interfacial boundary far into the bulk is *unexpected* because many amorphous polymer systems are theoretically well treated as van der Waals liquids with an interaction length on the order of the radius of gyration, i.e., the effective molecular size. At solid interfaces the radius of gyration is further compressed, like a pancake, and thus, any memory effects of the solid are expected to be even more reduced to a pinning regime of only 0.5 to 2 nm[23]. Within the pinning regime, it is commonly accepted that the material is structurally altered and exotic properties are expected. Outside the pinning regime, the polymer is expected to behave bulk-like. Experiments show however, that such scaling theories, i.e., mean-field theories, fail in describing the observed unique mesoscale properties because they do not consider effects that occur during the film coating process, e.g., rapid solvent evaporation. For instance, recent SFM experiments revealed that the spin coating process altered the structural properties of polyethylene-copropylene (PEP) at silicon interfaces due to anisotropic molecular diffusion that is caused by process-induced structural anisotropy.[24] The polymer structure at the interface affects properties such as the entanglement strength, illustrated in Figure 3, and thermal properties such as the glass transition temperature (see also Buenviaje et al. in *Kinetics of Constrained Systems*).[25]

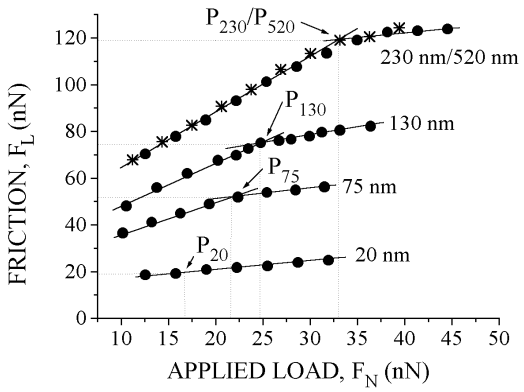

Figure 3. The transition point P_x (x = thickness of polymer film) corresponding to the discontinuity in the friction vs. loading curve is a measure of the entanglement strength of the polymer (polyethylene-copropylene). The bulk value is reached for films thicker than 230 nm. Films thinner than 230 nm are partially disentangled due to the spin coating process, and thus, the transition point occurs earlier. Within a 20 nm boundary regime, the film is entirely disentangled (gel-like). Reproduced with permission from reference 24. American Chemical Society, 1999.

Thermal annealing has been found inadequate to relax process-induced structural anisotropy for interfacially constrained PEP systems because of insufficient "mixing" at the interface [24] (see also below fractal kinetics at interfaces).

Interfacially Confined Liquids - above the critical threshold

Note that complex liquids like polymer solutions are different from thin polymer films. Interfacial effects have been found to exceed the molecular dimension by more than one order of magnitude.[26-28] Rheological properties of submicrometer thick liquids have been studied in the past quite successfully with surface force apparatus (SFA).[26-43] Montfort and Hadziioannou, for instance, confined nanometer thick films of long chain molecules between mica sheets and measured the static forces as the two SFA surfaces engaged each other[28]. As illustrated in Figure 4, repulsive forces were found to extend beyond separation distances of 10 times the radius of gyration, R_g, determined for the bulk. The steep repulsive slope in the force at small separation distances is due to a hard wall effect. The authors conclude, based on the high wetability of perfluorinated polyether used to clean mica surfaces, that the formation of surface films on each face plus unattached chains in between are causing the measured long-range repulsive forces.

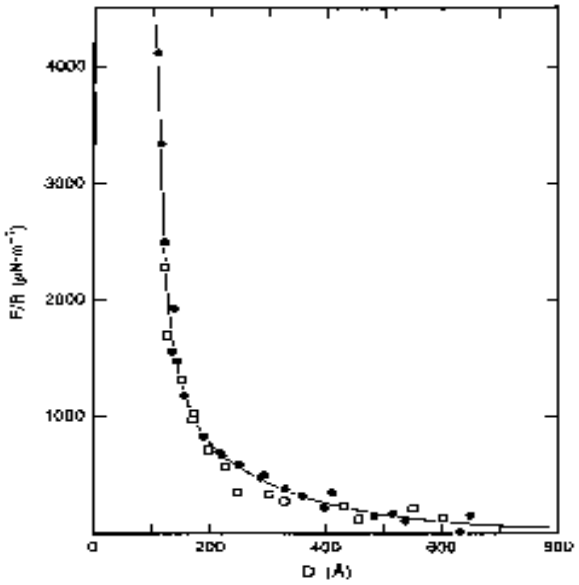

Figure 4. Logarithmic force/(radius of curvature) vs. distance, d, of perfluorinated polyether liquid at 25 ^oC (· droplet between the surfaces) (ð immersed surfaces in the liquid). Reprinted with permission from reference 28. American Institute of Physics, 1988.

Montfort and Hadziioannou also studied the effect of interfacial interactions, ie., surface forces, on the rheological

response of films as thin as 200 nm with sinusoidal modulated perturbation. They considered the following forces:

(a) the inertial force, $F_I = m\frac{d^2x}{dt}$,
(b) the restoring force of the spring, $F_R = -kx$,
(c) the surface forces, F_S,
(d) the hydrodynamic forces, F_H.

The surface forces were approximated from sinusoidal perturbation as:

$$F_S(D) = F_S\left(\overline{D}\right) + k_{eff} \times \left(D - \overline{D}\right), \qquad (2)$$

with the perturbation distance, D, around the mean distance, $\overline{D}$, and the effective spring constant, k_{eff}, that is determined from static force-distance measurements. k_{eff} is a measure of the effective stiffness of the systems including the sample liquid and the surface force apparatus. Repulsive forces are provided by $k_{eff}<0$. The hydrodynamic force, F_H, of the confined liquid has been treated by *Montfort* and *Hadziioannou* as a first-order linear, viscoelastic fluid by combining the continuity equation and the equation of motion for incompressible liquids with the Maxwell model. Based on this model, they obtained the following functional relationship between the relative response amplitude A' and k_{eff} (and k_{eff} /k) for a constant modulation frequency, ω, and a fixed geometry:

$$\frac{1}{A'} = \frac{\left[\frac{\omega\eta_o}{\alpha\left(1+\omega^2 t_o^{\,2}\right)}\right]^{-1}}{\sqrt{1+\left[\omega t_o + \alpha\left(1-\frac{k_{eff}}{k}\right)\frac{1+\omega^2 t_o^{\,2}}{\omega\eta_o}\right]^2}} \qquad (3)$$

$$\alpha = \frac{k\overline{D}}{6\pi R^2}$$

where the system relaxation time is t_o. Equation 3, illustrated in Figure 5, indicates that repulsive surface forces show a comparable and qualitatively similar response behavior to systems where no surface forces are present. For attractive surface forces, the qualitative behavior of A' strongly depends on the stiffness relationships between the system, both the spring and the liquid.

Montfort and *Hadziioannou* experimentally confirmed their macroscopic theory for perfluorinated polyether beyond a mean separation distance of approximately 200 nm.[28] Thus, phenomenological theories are found to predict well the viscoelastic behavior of semidilute polymer solutions up to a critical thickness where interfacial interactions become dominant.

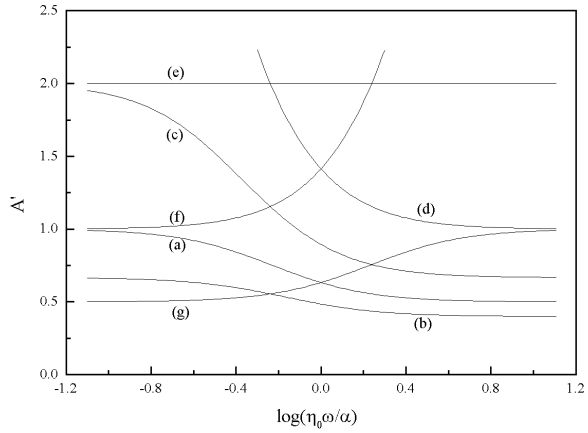

Figure 5. Amplitude of oscillations for a Maxwell fluid in the presence of surface forces: (a) $k_{eff}<0$, (b) no surface forces: $k_{eff}=0$, (c) $0<k_{eff}/k<1$, (d) $k_{eff}/k=1$, (e) $k_{eff}/k=1+G_o/\alpha$, (f) $k_{eff}/k>1+G_o/\alpha$; for $G_o/\alpha=1$. Reprinted with permission from reference 28. American Institute of Physics, 1988.

Interfacially Confined Liquids - below the critical threshold

Below a critical thickness of interfacially confined liquids, macroscopic phenomenological theories have to be adjusted. Simple nonpolar liquids such as hexadecane exhibit oscillarory solvation forces if compressed to a remaining film thickness of less than 4nm.[26] This phenomena had been described as freezing-melting transition and layering.[44] Grand canonical Monte Carlo and Molecular Dynamic (MD) simulations discussed the oscillatory solvation forces in terms of phase transitions and recrystallization.[45] Such interfacial "structuring" has been observed in linear alkanes and spherical shaped molecules, such as octamethylcyclotetrasiloxane (OMCTS) under extreme compression down to the few remaining molecular layers between the surfaces.[26,46]

To date there is no conclusive experimental evidence that the solvation forces in nonpolar liquids are indeed crystallization processes. *Gao* and *Landman* suggest with their MD simulation that the molecular surface corrugations are "imprinted" into the nanoconfined and highly pressured (MPa) liquid. Their simulation predicts that if the commensurability of the molecular surface corrugation of the two solid surfaces around the confined liquid of spherical shaped molecules is altered, e.g., incommensurable, the amplitude of the oscillatory solvation forces are reduced.[47] The theory of imprinted commensurable structures implies that the solvation forces of surface confined liquids should be drastically reduced for amorphous surfaces and for adjacent surfaces on the molecular dimension. O'Shea and Welland partially confirm this hypothesis with their SFM study on

OMCTS in which they observe oscillatory solvation forces only for very large blunt tips, 700 nm in diameter.

In general, the regime in which the solvation forces appear could be described as an entropically cooled boundary regime. The question arises if this boundary regime also exist without external pressure forces, i.e., solely because of surface interactions and a reduction in dimensionality. Winkler et al. predict with a MD simulation that hexadecane is well ordered, in crystalline like monolayers for strongly attractive surfaces.[48] In a very recent experimental study by Szuchmacher, He and Overney it was found by SFM shear modulation without applying external normal pressures, that there is an entropic cooling effect for hexadecane, illustrated in Figure 6, and for OMCTS at amorphous silicon-oxide surfaces.[49] A lateral modulation was chosen to avoid surface tapping and hydrodynamical damping in normal direction. The cantilever tip radius of curvature was estimated to be about 10-20 nm. A lateral modulation amplitude of 2 nm was chosen and an approach velocity of 0.5 nm/s was used. These small values guarantee a steady state approach.

In summary, we have discussed how interfacial effects can influence the viscoelastic properties of polymer coatings, polymer melts and solutes, and even simple nonpolar liquids within an interfacial boundary regime. In high molecular weight polymer systems, the interfacial boundary regime can reach up to hundreds of nanometers. The interfacial boundary layer of simple nonpolar fluids is restricted to a few nanometers. While outside the critical interfacial boundary layer interfacial effects on properties can be approached with phenomenological theories, modified or new theories are in demand within the structurally - or entropically cooled interfacial boundary layer. The modern theoretical approach of the fractal dimensionality will be discussed next.

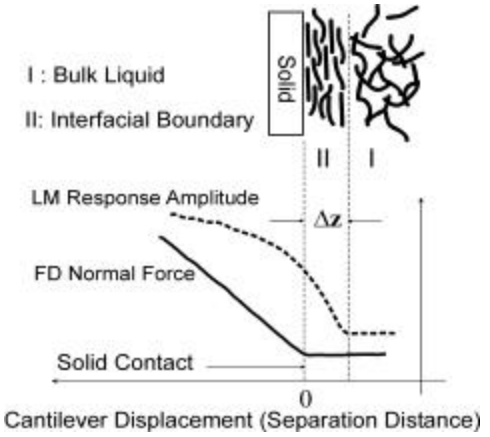

Figure 6. Interfacially confined hexadecane measured by SFM shear modulation spectroscopy. The shear response is measured simultaneously with the normal force deflection of the cantilever as function of the cantilever-siicon sample distance. The difference in the bending onset of the two curves defines the interfacially confined boundary layer thickness.

Critical Length Scales, Kinematics, and Dissipation

Dimensional and topological constraints

Critical length scales, kinematics and dissipation are primarily problems of distributions, probabilities, and cutoff limits.

Moving from two dimensional systems or nanoscale small ensembles to three dimensional systems, we will find ourselves in a fractional dimensionality. Material transport and reaction properties are known to be strongly affected by the so-called fractal dimension. For instance, for decades it is common knowledge that bulk kinetics and the kinetics at surfaces are significantly different processes. While bulk kinetics are described by time-independent rate constants, kinetics at surfaces reveal time dependent rate coefficients, also termed apparent coefficients [50]. Chemical and non-chemical, e.g., exciton-exciton recombination, reactions that take place at interfaces of different phases, are called *heterogeneous* reactions. Already in the late 1950s, the diffusion and the kinetics, for instance of the adsorption of alcohols at water-air interfaces, has been discussed in terms of barrier-limited adsorption [51] and diffusion-limited [52] processes with time-dependent reaction coefficients. The difference between a three-dimensional vs. a two-dimensional process is the degree of freedom. The degree of freedom limits the diffusive fluxes and hence, any kinetics in the absence of a convective process such as stirring. For chemical synthesis, this entropic cooling effect can be pictured as a constraint in the natural self-stirring process by diffusion.

Thus, dimensional constraints of surface reactions or topological constraints of solid-state reactions affect the nature and the strength of the transport mechanisms. It is important to note that underlying structural properties of the material might not be affected by these constraints. For chemical reactions the material properties will change over time if the products are incorporated in the interface. In that regard, the apparent material properties are favorably discussed in terms of transient thermodynamics.

Bulk processes which are not governed by a simple diffusion equation were found to yield time-dependent reaction coefficients. Briefly, diffusion controlled reactions between small molecules lead for two reactants to the following classical second order rate equation, Smoluchowski equation: [53]

$$\frac{\partial n_A}{\partial t} = \frac{\partial n_B}{\partial t} = -k n_A n_B; \quad k = 4\pi (D_A + D_B) b \qquad (4)$$

where the two species number densities are n_A and n_B, the two diffusion coefficients of the reactants are D_A and D_B, the capture or reaction radius is b, and the reaction rate constant is k. This equation is applicable to small molecule diffusion provided that the time $t \ll b^2/D_{AB}$, i.e., the diffusion length

$(D_{AB}t)^{1/2}$ exceeds the capture radius. However, macromolecules in melts or in concentrated solutions with attached flexible reacting groups show, for system relaxation times, or memory function, exceeding the process rates, a different rate equation of the form: [54]

$$\frac{\partial n_A}{\partial t} = \frac{\partial n_B}{\partial t} = -k(t) n_A n_B$$

$$k(t) = \frac{x^d(t)}{t} \frac{\sin(\pi u d)}{\sigma \pi} \qquad (5)$$

with a time dependent rate coefficient, where x(t) is the rms displacement of one monomer during a time *t*, *d* is the fractal dimension (for bulk d=3, for an ultrathin film, 2<d<3), *u* is the exponent of the memory function S(t) in form of a power law (u=1/2 for simple diffusion, i.e., $S(t) \sim t^{3/2}$ in three dimensions, and $x(t) \sim t^{1/2}$), and σ is the transport coefficient of the memory function ($\sigma = 2^{-3}\pi^{-3/2}$ for a Rouse chain with a reaction time smaller than the Rouse relaxation time of the chain). It is striking that besides the time dependence of the reaction rate coefficient in Eq. (5), *k* becomes essentially independent of the capture radius b for 0<b<x(t). This last statement also holds for noncompact explorations (fast decaying memory function) although the rate coefficient is again time independent.

Properties and critical time scales

Underlying material properties that were in the past predominantly determined by macroscopic experiments are microscopic transfer properties of momentum and energy. Microscopic transport mechanisms are governed by couplings between atoms or molecules, intra- and intermolecular degrees of freedom, and external forces. While for example, the dimensionality of the system, e.g., a two-dimensional surface vs. a three-dimensional body, significantly affects the intermolecular degrees of freedom of molecules. The intramolecular degrees of freedom are influenced by chemical groups and the stiffness of intramolecular chemical bonds.

Associated with couplings is a spectrum of intrinsic characteristic times, τ_i, and extrinsic characteristic times, τ_e, also called the operational "drive" time. With intrinsic characteristic times, it is referred to structural relaxation, energy distribution and dissipation times, and with extrinsic characteristic times it is pointed to operational dependent times that are connected to the rate of the applied external forces. The relationship between the two relaxation times (the ratio is called the Deborah number, D_e [55]) is critical for many processes.

In mechanical systems of confined rheological films with drive velocities that are comparable to material relaxation times, i.e., $D_e \sim 1$, new strategies have to be developed to avoid energy consuming resonance effects. In experiments that were concerned with modern *boundary* lubrication, where the lubricant film thickness is on the molecular length scale, the rate dependence of dissipative forces such as friction was illustratively documented.

Israelachvili and co-workers found that thin lubricant films can exhibit solid-like properties, including a critical yield stress and a dynamic shear melting transition, which can lead to stick-slip motions [34,35,56,57]. The generic shape of an overdamped stick-slip behavior is illustrated in Figure 7, which has been observed with SFA measurements as sketched in Figure 8 [57]. The spring force, F=-k(u-vt), results from the difference of the relative displacement of the block to the stationary lower surface, u, and the drive distance, vt, in conjunction with the spring constant k.

Yoshizawa and *Israelachvili* interpreted the stick-slip behavior at lower velocity as some sort of melting-freezing transition [57]. More accurately one could describe these two pseudo-states during a stick-slip cycle as transition phases in a dynamic process with high and low degrees of order, respectively. The less ordered or fluidized state was found to be increasingly important at higher velocities [58,59]. As it is illustrated in Figure 7, above a critical velocity, v_c, steady sliding is observed. Experimentally, *Yoshizawa, Chen* and *Israelachvili* [58], and theoretically, *Gao, Luedtke* and *Landman* [59], observed that at velocities even higher than v_c, eventually a state of ultralow kinetic friction occurs. *Landman* et al. observed this ultra-low friction regime also by lateral sinusoidal perturbation with small amplitudes (~1 Å) and high frequencies, which are related to the relaxation times in the material [59]. They found that at Deborah numbers of 0.75 and 7.5, stick-slip behavior and superkinetic sliding, respectively, dominated.

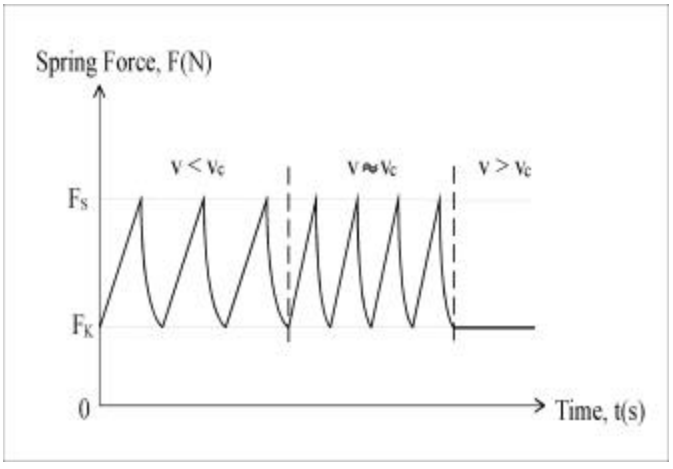

Figure 7. Illustration of a generic stick-slip motion of an overdamped spring system for increasing pulling velocities. Below the critical values for temperature, T_c, and shear rate, v_c, dominant stick-slip motions have been observed for hexadecane films [57]. The stick-slip spikes disappear as the velocity is increased above v_c. Reprinted with permission from reference 27. World Scientific, 1998.

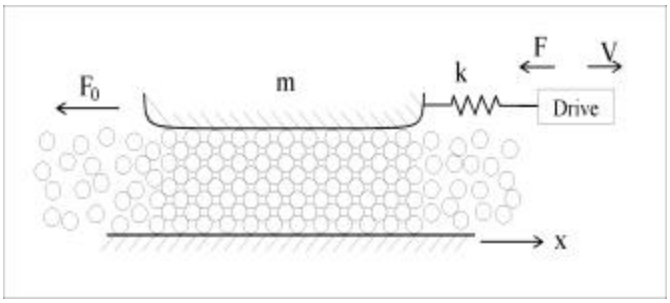

Figure 8: Mechanical analog of the SFA experimental setup used for measurements of friction forces F_o. A block of mass m which is confining a thin liquid film of hexadecane between atomically smooth mica is pulled laterally at velocity v. The lateral forces, F, are measured with an elastic spring of spring constant k [57]*. Reprinted with permission from reference 27. World Scientific, 1998.*

"Stick-slip" and dissipation

The stick-slip behavior discussed above, originates from dynamic order transitions of mechanically confined fluids. It should not be confused with the true molecular stick-slip behavior as theoretically predicted by Prandtl [60] and Tomlinson [61] at the beginning of the last century and experimentally confirmed towards the end of the century by scanning force microscopy [62].

Molecular or atomistic stick-slip was found to be the microscopic origin of dry friction where a single molecule or atom is dragged in contact over a molecularly structured surface. Briefly, the surface structure defines a corrugation potential along which the dragged atom moves, or more accurately, sticks and slips. The potential shape has to be considered relative to the position of the dragged atom, and is distorted if one considers surface elastic components. Thus, the potential stiffness, k_{pot} (second spatial derivative of the potential) has to be compared to the drag force stiffness, k_{drag} (first spatial derivative of the drag force). As long as $k_{pot} > k_{drag}$, the molecule or atom will "stick" to the surface. Its relative lateral motion is restricted to very small elastic distortions of the surface beneath. With increasing relative distortion of the potential, the potential stiffness is decreasing until at $k_{pot} = k_{drag}$, a sudden transition from sticking to slipping occurs. At this instability point, the dragged atom (molecule) will pop off the surface and slip until it dissipated enough energy so that it can be capture again by the surface beneath. Note that there is always a positive load applied between the dragged atom or molecule and the "sliding" surface. During the slip process, there is enough energy available to overcome the normal load component, and the dragged atom or molecule temporarily looses contact. Thus, the applied load is a crucial parameter for the stick-slip motion. Further, the qualitative behavior of the stick-slip motion, i.e., the slip distance, was found to depend on the drag velocity [62]. At very low drag velocities (~1nm/s), the slip distance was found to correspond to the lattice distance of the structured surface, Figure 9.

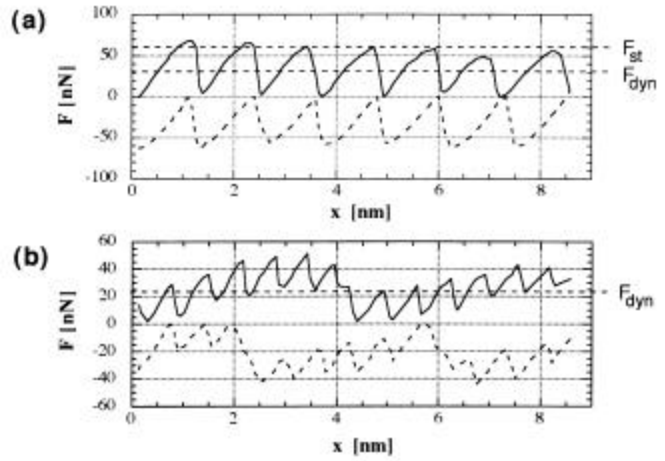

Figure 9. Molecular stick-slip behavior measured on anisotropic, row-like, surface lattice of a lipid film at a drag velocity of 1 nm/s. (a) Sliding direction perpendicular to the row-like structure, (b) sliding direction 60° to the row-like structure. Reprinted with permission from reference 62. The American Physical Society, 1994.

At higher but still very slow drag velocities (~100 nm/s), the slip distance increased and changed its regular pattern to become more erratic.

During the slip-process, energy is dissipated in the form of vibrations. The terminology of "dissipative vibrations" implies an entropically driven atomistic or molecular uncoordinated process (stochastic, chaotic). In other words, the dissipation is a form of energy transformation from a lower dimensionality to a higher dimensionality, i.e., a 2D frictional interface to a 3D bulk material. The slip-process is irreversible because the probability for reverse-energy-transfer is unlikely; i.e., a reversed energy transfer would require a highly improbable collective process of all vibrating molecules leading to a reduced entropy state. The unlikeness of the reversed process is illustrated with the following *Gedanken*-experiment:

A non-moving solid, which is connected to a spring, on a horizontal plane is heated up from an initial temperature T_i to an elevated temperature T_f. It is assumed that the structural integrity is maintained and that, with adiabatic boundary conditions, all energy due to a constant heat rate is stored as vibrational energy in the solid. If molecular friction as described above were reversible, there would be a high probability that the solid starts moving in a particular direction as if pulled, and thus would exert a force on the spring. Hence, frictional reversibility would imply that thermal energy can be reversibly transformed into mechanical energy, which contradicts the second law of thermodynamics. There is an

interesting aspect to this *Gedanken*-experiment, if one considers the sliding direction. Frictional sliding is well directed in one dimension. The sliding process in the *Gedanken*-experiment could however occur in any direction on the two-dimensional (2D) plane over any time interval, i.e., it could resemble Brownian motion on a plane. Let us discuss what would happen if vibrational motion in two-dimensions could be transformed into 2D Brownian motion. If we collapse the solid to a single atom, the degree of vibrational freedom would not be three, but two because we would have to deduct one degree of freedom for the constraining surface. Thus, for a single molecule, the vibrational motion is like the 2D Brownian motion. If we consider a molecularly thick planar horizontal sheet as our solid, the observed 2D Brownian motion results from the weighted average of the 2D-constrained vibrating sheet-molecules. Thus as long as the vibrating molecules do not vibrate in registry, the thermal energy stored could not be extracted by the attached spring.

At that point, the question arises if it is desirable to intentionally activate vibrational modes in the solid that show a high degree of coordination. It is not because it opens up other gateways for energy dissipation, e.g., acoustic activation due to frictional sliding. Thus, as discussed above for lubricated sliding or dry sliding, the stick-slip phenomena has to be depressed to reduce dissipation. A way to depress the stick-slip behavior is to control either, chemical interactions by embedding surface inhomogeneities, or one of the most crucial parameters, the applied load. This topic is further discussed in *Finite Size Systems*. Porto, Urbakh and Klafter introduce novel modes of friction that are based on modifying imaginary shear modes; the *shearons.*

Closing Remarks

Reduced dimensionality paired with interfacial interactions were discussed as the major source for constraints in mesoscale systems. Material constraints leading to the observation of exotic properties were documented and illustrated from various fields. Although on first sight, the findings from the different disciplines appeared to be unrelated, they can be interpreted on a similar basis with the proposed classification of interfacial sciences.

To develop a unifying theory of Interfacial Mesoscale Sciences, it is necessary, as a combined effort, to classify the field. The classification presented here represents a first step. We urge the reader to reflect on this when reading the subsequent contributed chapters **.**

References

(1) Abbott, E. A. *Flatland - A Romance of Many Dimensions*; Dover Publ.: New York, 1992.

(2) Love, A. E. H. *A treatise on the mathematical theory of elasticity*; 4 ed.; Dover Publ.: New York, 1927.

(3) Jeans, J. H. *Roy. Soc. Proc. (Ser.A)* **1923**, *102*, 554.

(4) Tissue, B. M. *Chem. Mater.* **1998**, *10*, 2837.

(5) Goldburt, E. T.; Kulkarni, B.; Bhargava, R. N.; Taylor, J.; Libera, M. *J. Lumin.* **1997**, *72/74*, 190.

(6) Chen, X. L.; Jenekhe, S. A. *Macromolecules* **1996**, *29*, 6189-6192.

(7) Jenekhe, S. A.; Zhang, X.; Chen, X. L. *Chem. Mater.* **1997**, *9*, 409-412.

(8) Osaheni, J. A.; Jenekhe, S. A.; Perlstein, J. *J. Phys. Chem.* **1994**, *98*, 12727-12736.

(9) Zhang, X.; Jenekhe, S. A.; Perlstein, J. *Chem. Mater.* **1996**, *8*, 1571-1574.

(10) Bhargava, R. N. *J. Lumin.* **1996**, *70*, 85.

(11) Wolf, D.; Wang, J.; Phillpot, S. R.; Gleiter, H. *Phys. Rev. Lett.* **1995**, *74*, 4686.

(12) Itoh, T.; Furumiya, M. *J. Lumin.* **1991**, 704.

(13) Takagahara, T. *J. Lumin.* **1996**, *70*, 129.

(14) Wright, J. C. *Amorph. Mater.* **1985**, *12*, 505.

(15) G.A., W.; Beeson, K. W. *J. Mater. Res.* **1990**, *5*, 1573.

(16) Liu, Y.; Russell, T. P.; Samant, M. G.; Stohr, J.; Brown, H. R.; CossyFavre, A.; Diaz, J. *Macromolecules* **1997**, *30*, 7768-7771.

(17) Frank, B.; Gast, A. P.; Russel, T. P.; Brown, H. R.; Hawker, C. *Macromolecules* **1996**, *29*, 6531-6534.

(18) Overney, R. M.; Guo, L.; Totsuka, H.; Rafailovich, M.; Sokolov, J.; Schwarz, S. A. *Interfacially confined polymeric systems studied by atomic force microscopy*; Material Research Society:, 1997.

(19) Rabeony, M.; Pfeiffer, D. G.; Behal, S. K.; Disko, M.; Dozier, W. D.; Thiyagarajan, P.; Lin, M. Y. *J. Che. Soc. Faraday Trans.* **1995**, *91*, 2855-61.

(20) Green, P. F.; Christensen, T. M.; Russel, T. P.; Jérôme, J. J. *J. Chem. Phys.* **1990**, *92*, 1478.

(21) Russel, T. P.; Menelle, A.; Anastasiadis, S. H.; Satija, S. K.; Majkrzak, C. F. *Macromolecules* **1991**, *24*, 6263.

(22) Zheng, X.; Rafailovich, M. H.; Sokolov, J.; Strzhemechny, Y.; Schwarz, S. A.; Sauer, B. B.; Rubinstein, M. *Phys. Rev. Lett.* **1997**, *79*, 241-244.

(23) Brogley, M.; Bistac, S.; J., S. *Macromol. Theor. Simul.* **1998**, *7*, 65-68.

(24) Buenviaje, C.; Ge, S.; Rafailovich, M.; Sokolov, J.; Drake, J. M.; Overney, R. M. *Langmuir* **1999**, in press.

(25) Overney, R. M.; Buenviaje, C.; Luginbuehl, R.; Dinelli, F. *J. Thermal Anal. and Cal.* **2000**, in press.

(26) Israelachvili, J. N. *Intermolecular and Surface Forces, 2nd Ed.*; Academic Press:, 1992.

(27) Meyer, E.; Overney, R. M.; Dransfeld, K.; Gyalog, T. *Nanoscience, Friction and Rheology on the Nanometer Scale*; World Scientific: Singapore, 1998.
(28) Montfort, J. P.; Hadziioannou, G. *J. Chem. Phys.* **1988**, *88*, 7187-7196.
(29) Israelachvili, J. N. *Pure & App. Chem.* **1988**, *60*, 1473.
(30) Israelachvili, J. N.; Kott, S. J.; Fetters, L. J. *J. Polym. Sci., Phys. Ed.* **1989**, *27*, 489.
(31) Klein, J.; Kamiyama, Y.; Yoshizawa, H.; Israelachvili, J. N.; Fredrickson, G. H.; Pincus, P.; Fetters, L. J. *Macromolecules* **1993**, *26*, 5552.
(32) Luengo, G.; Schmitt, F.-J.; Israelachvili, J. *Macromolecules* **1997**, *30*, 2482-2494.
(33) Thompson, P. A.; Robbins, M. O.; Grest, G. S. *Israel J. Chem.* **1995**, *35*, 93.
(34) Yoshizawa, H.; McGuiggan, P.; Israelachvili, J. N. *Science* **1993**, *259*, 1305.
(35) Gee, M. L.; McGuiggan, P. M.; Israelachvili, J. N.; Homola, A. M. *J. Chem. Phys.* **1990**, *93*, 1895.
(36) Christenson, H. K.; Gruen, D. W. R.; Horn, R. G.; Israelachvili, J. N. *J. Chem. Phys.* **1987**, *87*, 1834-41.
(37) Cho, Y. K.; Dhinojwala, A.; Granick, S. *J. Polymer Sci. Part B - Polymer Physics* **1997**, *35*, 2961-2968.
(38) Granick, S. *Science* **1991**, *253*, 1374.
(39) Granick, S.; Hu, H.-W. *Langmuir* **1994**, *9*, 1983.
(40) Granick, S. *MRS Bulletin* **1996**, *21*, 33-6.
(41) Hu, H.-W.; Carson, G. A.; Granick, S. *Phys. Rev. Lett.* **1991**, *66*, 2758.
(42) Hu, H.-W.; Granick, S. *Science* **1992**, *258*, 1339.
(43) Reiten, G.; Demirel, A. L.; Peanasky, J.; Cai, L. L.; Granick, S. **199**.
(44) Israelachvili, J.; McGuiggan, P.; Gee, M.; Homola, A.; Robbins, M.; Thompson, P. *J. Phys.-Cond. Matter* **1990**, *2*, SA89.
(45) Bordarier, P.; Rousseau, B.; A.H., F. *Molecular Simulation* **1996**, *17*, 199.
(46) O'Shea, S. J.; Welland, M. E. *Langmuir* **1998**, *14*, 4186.
(47) Gao, J. P.; Landman, U. *Phys. Rev. Lett.* **1997**, *79*, 705.
(48) Winkler, R. G.; Schmid, R. H.; Gerstmair, A.; Reineker, P. *J. Chem. Phys.* **1996**, *104*, 8103.
(49) He, M.; Szuchmacher, A.; Overney, R. M. *in preparation* **2000**.
(50) Kopelman, R. *Science* **1988**, *241*, 1620.
(51) Hansen, R. S.; Wallace, T. C *J. Phys. Chem.* **1959**, *63*, 1085.
(52) Defay, R.; Hommelen, J. R. *J. Colloid. Sci.* **1959**, *14*, 411.
(53) Von Smoloushowski, M. *Z. Phys. Chem.* **1917**, *92*, 192.
(54) de Gennes, P. G. *J. Chem. Phys.* **1981**, *76*, 3316.
(55) Reiner, M. *Phys. Today* **1964**, *January*, 62.
(56) Israelachvili, J. N. *Science* **1988**, *240*, 189.
(57) Yoshizawa, H.; Israelachvili, J. N. *J. Phys. Chem.* **1993**, *97*, 11300.
(58) Yoshizawa, H.; Chen, Y.-L.; Israelachvili, J. N. *Weat* **1993**, *168*, 161.
(59) Gao, J.; Luedtke, W. D.; Landman, U. *J. Phys. Chem. B* **1998**, *102*, 5033.
(60) Prandtl, L. *Z. Angew. Math. Mechanik* **1928**, *8*, 85.
(61) Tomlinson, G. A. *Phil. Mag.* **1929**, *7*, 905.
(62) Overney, R. M.; Takano, H.; Fujihira, M.; Paulus, W.; Ringsdorf, H. *Phys. Rev. Lett.* **1994**, *72*, 3546-49.